Acta Cryst. (1992). B48, 782–789

Molecular Structure and Crystal Packing of 6-(*p*-Dimethylaminophenyl)fulvene

BY LAVINIA M. WINGERT* AND STUART W. STALEY†

Department of Chemistry, Carnegie Mellon University, 4400 Fifth Avenue, Pittsburgh, PA 15213, USA

(*Received* 5 *August* 1991; *accepted* 21 *January* 1992)

Abstract

The single-crystal structure of 6-(*p*-dimethylaminophenyl)fulvene (DMAPF), $C_{14}H_{15}N$, $M_r = 197.28$, $F(000) = 848$, at 123 K has been determined and refined from Mo $K\alpha$ ($\lambda = 0.7107$ Å) X-ray data collected up to $\sin\theta/\lambda = 0.7$ Å^{-1}. Monoclinic, $P2_1/c$, $Z = 8$. At 123 K: $a = 10.989$ (2), $b = 7.847$ (2), $c = 25.833$ (4) Å, $\beta = 103.61$ (2)°, $V = 2.165$ (10) Å^3. At 293 K: $a = 11.085$ (3), $b = 8.035$ (2), $c = 26.006$ (8) Å, $\beta = 103.58$ (2)°, $V = 2.252$ (13) Å^3. The structure was refined using 6459 unique reflections to a final wR of 5.89% with anisotropic temperature factors on non-H atoms, isotropic temperature factors on H atoms, and populations of radial electron density distributions on every atom as variables in the refinement. All reflections were treated as observed. In both molecules of the asymmetric unit the dihedral angle between the benzenoid and fulvene rings is approximately 15°, whereas pyramidalization at the N atom is 2.5 times greater in one molecule than in the other. The crystal structure is composed of layers parallel to the *ab* plane with molecules aligned in the *c* direction. The molecules of each layer pack with their cross-sections forming a herringbone pattern. Comparison of geometric and electronic features of crystalline DMAPF with those derived by molecular orbital calculations indicate enhanced polarization due to the crystal field.

Introduction

This crystallographic report is part of a larger study of substituent and environmental effects on highly polarizable molecules, in particular 6-arylfulvenes and 6-methyl-6-arylfulvenes. These compounds are of interest because of the properties of the fulvene subunit, such as its polarizability and electron-withdrawing ability.

Fulvene is not intrinsically a highly polar molecule. Its dipole moment in the gas phase (0.42 D; 1 D $\simeq 3.33564 \times 10^{-30}$ C m) (Baron, Brown, Burden, Domaille & Kent, 1972) is essentially identical to that of cyclopentadiene (Scharpen & Laurie, 1965). A high level of electron correlation is required in order to reproduce the fulvene value theoretically (Replogle, Trucks & Staley, 1991).

There is ample evidence that fulvene and 6-aryl-substituted fulvenes are quite *polarizable*. Polarizability is manifested by a change in the dipole moment on altering either the environment or a substituent. Thus, the dipole moment of fulvene was determined to be 1.1 D in benzene solution (Thiec & Wiemann, 1956) and estimated from the dipole moment of 6,6-diphenylfulvene in benzene (Wheland & Mann, 1949) to be 1.2 D, values considerably higher than the 0.42 D value measured in the gas phase. Furthermore, Kresze & Goetz (1957) have determined the dipole moment of *p*-(dimethylaminophenyl)fulvene (DMAPF) (1) in benzene to be 3.65 D and have estimated a minimum enhancement of 1.14 D relative to the sum of the moments of the fulvene and *N*,*N*-dimethylaniline components. The solution dipole moment of DMAPF is also enhanced over a value of 2.8 D calculated by molecular orbital theory (Ikeda, Kawabe, Sakai & Kawasaki, 1989). The latter probably corresponds to a gas-phase value but the molecular geometry for the calculation was not reported. These authors have concluded that resonance interactions of the fulvene group in DMAPF produce nonlinear optical responses comparable to those of strong electron-withdrawing groups such as β-nitrovinyl and β,β-dicyanovinyl.

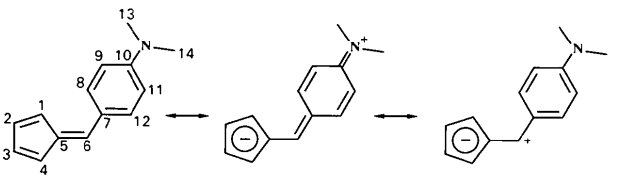

Polarization of 6-arylfulvenes (Otter, Mühle, Neuenschwander & Kellerhals, 1979; Bönzli, Otter, Neuenschwander, Huber & Kellerhals, 1986) and 6-methyl-6-arylfulvenes (Sardella, Keane & Lemonias, 1984) has also been investigated by ^{1}H and ^{13}C NMR spectroscopy. Resonance effects in the latter series are attenuated by a twisting of the benzenoid ring relative to the fulvene ring. However, the ^{13}C chemical shifts of a series of 6-arylfulvenes, including

* Present address: Department of Crystallography, University of Pittsburgh, Pittsburgh, PA 15260, USA.

† Author for correspondence.

0108-7681/92/060782-08$06.00

DMAPF (Bönzli *et al.*, 1986), clearly show a strong contribution of resonance forms (1*a*) and/or (1*b*) to the ground state.

Experimental and computational methods

Crystal structure determination

DMAPF was prepared by the classical Thiele synthesis (Thiele, 1900; Thiele & Balhorn, 1906; Kresze & Goetz, 1957; Otter *et al.*, 1979) and recrystallized from hexane. Crystals of DMAPF belong to the monoclinic space group $P2_1/c$, as determined by precession photography. The red–orange crystals are plate-like, and developed on {001} with a density of 1.162 g cm^{-3} as measured by flotation. A crystal with dimensions 0.42 × 0.44 × 0.36 mm, in the *a*, *b* and *c** directions respectively, was chosen for data collection. Cell dimensions at 293 and 123 K were refined by least-squares fitting to θ settings for 25 centered reflections ($\theta > 16°$) on an Enraf–Nonius CAD-4 diffractometer with Mo $K\alpha$ radiation (λ = 0.7107 Å). Intensity profiles of 7364 reflections were measured at 123 K by $\theta/2\theta$ scans in the $+h$, $+k$, $\pm l$ quadrant of reciprocal space with $0 \le h \le 15$, $0 \le k \le 11$, $-36 \le l \le 32$ and $2.5 < \theta < 30°$ ($0.06 < \sin\theta/\lambda < 0.70$ Å^{-1}). The average intensity of three standards ($3,0,\bar{1}2$; $\bar{2}\bar{4}2$; $4\bar{3}1$) varied from 101 to 90% of their average starting value. After averaging equivalent reflections (R_{int} = 2.5%) and removing systematic absences, the data set contained 6463 reflections. Carbon and nitrogen atomic positions of two symmetry-independent molecules (*A* and *B*) were determined by use of the direct-methods program, *MULTAN*78 (Main, Hull, Lessinger, Germain, Declercq & Woolfson, 1978). H atoms were located by difference Fourier mapping.

In the data processing, background corrections were based on least-squares fitting to intensity profiles outside peak limits set by the method of Lehmann & Larsen (1974). Processing was carried out by a series of programs developed at the Buffalo Medical Foundation: *REFPK*, *BGLP*, *SCALE*3 (Blessing, 1987) and *ABSORB* (DeTitta, 1985). With μ = 0.7296 cm^{-1}, the maximum and minimum transmission factors were 0.981 and 0.974, respectively. By use of an interactive program *BROWSE* (Spackman, 1987), the absorption edge of the β-filter was found to lie *within* the scan limits for 46 low-angle reflections ($\theta < 10°$), resulting in underestimation of the background. The low-angle scan limit was therefore shifted to exclude the absorption edge in determining background corrections for these reflections.

Least-squares refinement of the DMAPF crystal structure was carried out on *F* by use of the *VALLSQ* subroutine of the program *VALRAY* (Stewart & Spackman, 1983). The scattering factors used by the program are constructed from exponential radial functions that depend on the model chosen. In the refinement of the DMAPF crystal structure, the model used was the independent atom model (IAM) in which the scattering factors reproduce a Hartree–Fock function for each atom. The radial exponents, α, were held constant at standard values: 3.90 bohr^{-1} for N, 3.44 bohr^{-1} for C and 2.48 bohr^{-1} for H (1 bohr ~ 5.292 × 10^{-11} m). No reflections were treated as unobserved.

In the initial cycles of this 60-atom refinement, 390 positional and thermal parameters were refined, anisotropically on carbons and nitrogens and isotropically on hydrogens. No extinction correction was applied. However, four reflections ($21\bar{1}$, 210, 220 and 021) strongly affected by extinction were removed. Refinement of the 390 positional and thermal parameters converged with $wR(F)$ = 6.20% using 6459 unique reflections with $\sin\theta/\lambda \le 0.7$ Å^{-1}. A parallel refinement limiting the data to the 1230 reflections with $\sin\theta/\lambda \le 0.4$ Å^{-1} resulted in $wR(F)$ = 4.65%. In order to carry out refinement of atomic electron populations, the larger data set with higher resolution ($\sin\theta/\lambda \le 0.7$ Å^{-1}) was used. With the addition of one electron population parameter per atom, 450 parameters were refined to a final $wR(F)$ = 5.89% with $w = 1/\sigma$. In the final cycle of refinement, the maximum shift/σ = 0.003. In the final difference Fourier map, $-0.59 < \Delta\rho < +0.71$ e Å^{-3}.

Molecular orbital calculations

The *GAUSSIAN*88 program package (Frisch *et al.*, 1988) was used with the STO-3G basis set (Hehre, Stewart & Pople, 1969; Hehre, Ditchfield, Stewart & Pople, 1970) to *fully* optimize the DMAPF structure and to calculate the electronic structure of DMAPF molecules *A* and *B* with *crystal geometry* at the Hartree–Fock (HF) level. *Crystal geometry* herein refers to the parameters refined by diffraction data except for the C—H bond lengths, which have been optimized at the HF/STO-3G level. This optimization was carried out because C—H bond lengths determined by X-ray diffraction are shorter than the corresponding internuclear distances due to the shifting of hydrogen electron density away from the nucleus in the direction of the C—H bond. The optimization of the DMAPF molecule employed analytically evaluated atomic forces in a multiparameter search routine (Schlegel, 1982) and was carried out in stages that encompassed (1) all bond lengths, (2) all non-H parameters and (3) all parameters. Analytical frequency analysis confirmed that the final optimized structure is a true energy minimum. Fulvene π charges were estimated from

Mulliken $2p_y$ orbital populations obtained with the y axis set perpendicular to the plane of atoms C3, C4 and C5 of the fulvene ring. Similarly, aryl π charges were estimated from calculations in which the y axis was set perpendicular to the plane of three atoms of the aryl ring.

Results

Geometric and electronic features

Refined cell dimensions at 293 and 123 K are given in Table 1 along with other crystal data. Fractional atomic coordinates for the DMAPF crystal structures are listed in Table 2 along with isotropic thermal parameters (B for hydrogens and B_{eq} for non-hydrogens) and electron populations determined by least-squares refinement.* An *ORTEP* (Johnson, 1976) drawing of one molecule is shown in Fig. 1 with atomic numbering and thermal ellipsoids at the 50% probability level. Fig. 2 presents *ORTEP* drawings of two views of the crystal packing with 20% probability ellipsoids. Bond lengths, valence angles and torsion angles involving adjacent heavy atoms are listed in Tables 3, 4 and 5, with atoms numbered as in Fig. 1. In order to facilitate comparison of molecules A and B, the torsion angles for B listed in Table 5 refer to the enantiomorph ($-x$, $-y$, $-z$). Key geometric features, including angles between least-squares planes, pyramidalization at the N atom and averages of selected bond lengths are given in Table 6. Corresponding values for the fully optimized HF/STO-3G molecular orbital structure of DMAPF are also given in Tables 3–6. Total and π atomic charges derived from *ab initio* HF/STO-3G molecular orbital calculations for the crystal and optimized geometries of DMAPF are listed in Table 7, along with dipole moments calculated at the same level.

Crystal packing

In the DMAPF crystal, molecules align lengthwise along the c axis in layers that lie parallel to the ab plane (perpendicular to c^*). With $\beta = 103.6°$, the molecules are tilted 13.6° (the angle between c and c^*) from the normal to the layer planes (Fig. 2*a*). Each unit cell contains eight molecules and spans two layers. Intermolecular C···H and N···H distances of less than 3 Å are given in Table 8. There are 16 such distances between each A molecule and its neighbors involving 11 non-H atoms of A (first column of Table 8) and 5 H atoms of A (second column). There are 22 distances for each B molecule involving 8 non-H atoms and 14 H atoms (Table 8). There are no C···H or N···H distances < 3 Å between layers. The packing in one layer is also shown in Fig. 3 by a schematic drawing in which the molecules are viewed end-on and the cross section of each molecule is represented by an oval-shaped outline. In the figure, numbers of C···H and N···H distances of less than 3 Å are indicated. Ovals representing molecules with the dimethylamino group oriented toward the

Table 1. *Crystallographic data for dimethylaminophenylfulvene (DMAPF)*

Cell constants at 293 K:	a (Å)	11.085 (3)
	b (Å)	8.035 (2)
	c (Å)	26.006 (8)
	β (°)	103.58 (2)
	V (Å^3)	2252 (13)
Cell constants at 123 K:	a (Å)	10.989 (2)
	b (Å)	7.847 (2)
	c (Å)	25.833 (4)
	β (°)	103.61 (2)
	V (Å^3)	2165 (10)
D_x [a] (g cm^{-3})		1.164
D_m [a] (g cm^{-3})		1.162
μ(Mo $K\alpha$)[a,b] (cm^{-1})		0.7296
Crystal size (mm)		0.42 × 0.44 × 0.36
Formula		$C_{14}H_{15}N$
Molecular weight		197.28
Space group		$P2_1c$
Z (molecules/unit cell)		8
F(000)		848
Diffractometer		Enraf Nonius CAD-4
Radiation		Mo $K\alpha$, λ = 0.7107 Å
Number of measured reflections		7364
Number of unique reflections		6463
Number of reflections used in refinement		6459
R (%)		14.57
wR (%)		5.89
S		1.77

Notes: (*a*) At room temperature, 293 K. (*b*) The linear absorption coefficient, μ, applied here is calculated from mass absorption coefficients in the *International Tables for X-ray Crystallography*, Vol. III, p. 162. Using values from Vol. IV, p. 61, the calculated value of μ is 0.6291 cm^{-1}.

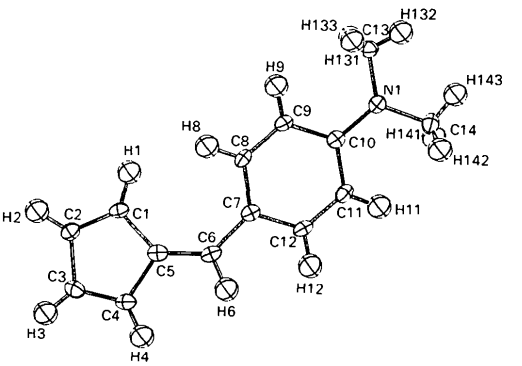

Fig. 1. 6-(*p*-Dimethylaminophenyl)fulvene (molecule B, $-x$, $-y$, $-z$ coordinates) at 123 K with thermal ellipsoids at the 50% probability level and hydrogen thermal parameters fixed at B = 3.0 Å^2 (Johnson, 1976). Atomic numbering is that used in the text.

* Lists of structure factors for all data, including those omitted due to extinction, and anisotropic thermal parameters have been deposited with the British Library Document Supply Centre as Supplementary Publication No. SUP 54905 (45 pp.). Copies may be obtained through The Technical Editor, International Union of Crystallography, 5 Abbey Square, Chester CH1 2HU, England. [CIF reference: GR0192]

Table 2. *Refined parameters of the DMAPF crystal structure*

Estimated standard deviations, in parentheses, apply to the least significant digit. Atoms are numbered as in Fig. 1.

	x	y	z	B_{eq}/B[a]	Electron population[b]
Molecule *A*					
C1	0.2083 (2)	0.2013 (2)	0.8962 (1)	1.91 (5)	5.92 (5)
C2	0.2252 (2)	0.2175 (3)	0.9498 (1)	2.23 (5)	5.99 (5)
C3	0.1316 (2)	0.1159 (3)	0.9673 (1)	2.35 (5)	5.80 (5)
C4	0.0577 (2)	0.0408 (3)	0.9247 (1)	2.24 (5)	6.04 (5)
C5	0.1018 (2)	0.0874 (2)	0.8772 (1)	1.90 (5)	6.25 (5)
C6	0.0454 (2)	0.0274 (2)	0.8279 (1)	1.96 (5)	6.03 (5)
C7	0.0745 (1)	0.0491 (2)	0.7763 (1)	1.78 (5)	6.29 (5)
C8	0.1870 (2)	0.1148 (2)	0.7674 (1)	1.84 (5)	6.13 (5)
C9	0.2050 (2)	0.1345 (2)	0.7169 (1)	1.82 (5)	5.97 (5)
C10	0.1109 (2)	0.0888 (2)	0.6714 (1)	1.69 (5)	6.06 (5)
C11	−0.0013 (2)	0.0199 (2)	0.6801 (1)	1.96 (5)	5.91 (5)
C12	−0.0174 (2)	−0.0000 (2)	0.7307 (1)	2.01 (5)	5.80 (5)
C13	0.2361 (2)	0.1994 (4)	0.6122 (1)	2.28 (5)	5.46 (7)
C14	0.0247 (2)	0.0729 (3)	0.5752 (1)	2.21 (5)	5.38 (7)
N1	0.1278 (1)	0.1083 (2)	0.6207 (1)	2.14 (4)	7.09 (4)
H1	0.257 (2)	0.261 (2)	0.873 (1)	3.8 (7)	0.99 (5)
H2	0.287 (2)	0.287 (3)	0.972 (1)	4.7 (7)	1.08 (5)
H3	0.124 (2)	0.110 (2)	1.002 (1)	4.4 (7)	1.08 (5)
H4	−0.017 (2)	−0.041 (3)	0.924 (1)	3.0 (7)	0.85 (5)
H6	−0.029 (2)	−0.046 (2)	0.827 (1)	0.4 (5)	0.72 (4)
H8	0.253 (2)	0.146 (2)	0.798 (1)	5.5 (7)	1.23 (5)
H9	0.284 (2)	0.182 (2)	0.712 (1)	3.3 (6)	1.01 (5)
H11	−0.067 (2)	−0.010 (2)	0.651 (1)	3.1 (6)	0.95 (5)
H12	−0.096 (2)	−0.044 (3)	0.735 (1)	2.7 (7)	0.84 (5)
H131	0.232 (2)	0.196 (2)	0.577 (1)	5.8 (7)	1.21 (6)
H132	0.313 (2)	0.145 (3)	0.631 (1)	4.8 (7)	1.06 (5)
H133	0.239 (2)	0.309 (4)	0.624 (1)	5.4 (8)	1.08 (6)
H141	0.054 (2)	0.091 (2)	0.544 (1)	7.4 (7)	1.41 (6)
H142	−0.046 (2)	0.140 (3)	0.576 (1)	5.3 (7)	1.16 (5)
H143	0.004 (2)	−0.043 (3)	0.575 (1)	5.6 (7)	1.21 (6)
Molecule *B*					
C1	0.6924 (2)	0.2092 (2)	0.6538 (1)	1.67 (4)	6.04 (5)
C2	0.6878 (2)	0.2305 (3)	0.6012 (1)	1.84 (5)	6.00 (5)
C3	0.5979 (2)	0.1094 (2)	0.5706 (1)	2.04 (5)	5.99 (5)
C4	0.5496 (2)	0.0161 (3)	0.6044 (1)	1.94 (5)	6.06 (5)
C5	0.6051 (1)	0.0734 (2)	0.6592 (1)	1.60 (4)	6.29 (5)
C6	0.5672 (2)	0.0089 (2)	0.7018 (1)	1.64 (4)	6.02 (5)
C7	0.5997 (1)	0.0513 (2)	0.7583 (1)	1.47 (4)	6.25 (5)
C8	0.7004 (2)	0.1536 (2)	0.7852 (1)	1.54 (4)	6.02 (5)
C9	0.7214 (2)	0.1872 (2)	0.8389 (1)	1.57 (4)	5.94 (5)
C10	0.6419 (1)	0.1196 (2)	0.8698 (1)	1.54 (4)	6.03 (5)
C11	0.5396 (2)	0.0191 (2)	0.8431 (1)	1.70 (5)	6.02 (5)
C12	0.5215 (2)	−0.0146 (2)	0.7896 (1)	1.64 (4)	5.87 (5)
C13	0.7627 (2)	0.2594 (3)	0.9509 (1)	1.91 (5)	5.34 (7)
C14	0.5819 (2)	0.0702 (3)	0.9541 (1)	2.01 (5)	5.52 (7)
N1	0.6645 (1)	0.1457 (2)	0.9239 (1)	1.92 (4)	6.96 (4)
H1	0.744 (2)	0.276 (2)	0.684 (1)	4.6 (6)	1.13 (5)
H2	0.739 (2)	0.316 (3)	0.586 (1)	2.9 (6)	0.94 (4)
H3	0.579 (2)	0.099 (2)	0.532 (1)	6.7 (7)	1.29 (6)
H4	0.488 (2)	−0.076 (3)	0.597 (1)	2.6 (6)	0.93 (4)
H6	0.501 (2)	−0.076 (2)	0.693 (1)	2.2 (5)	0.95 (4)
H8	0.756 (2)	0.203 (2)	0.764 (1)	3.7 (6)	1.13 (5)
H9	0.792 (2)	0.257 (3)	0.856 (1)	1.7 (6)	0.80 (4)
H11	0.483 (2)	−0.030 (2)	0.863 (1)	2.1 (6)	0.88 (4)
H12	0.454 (2)	−0.089 (2)	0.773 (1)	1.8 (5)	0.90 (4)
H131	0.747 (2)	0.370 (4)	0.940 (1)	6.0 (8)	1.10 (6)
H132	0.767 (2)	0.257 (3)	0.987 (1)	7.0 (8)	1.23 (6)
H133	0.838 (2)	0.223 (3)	0.946 (1)	4.6 (7)	1.06 (5)
H141	0.573 (2)	−0.047 (3)	0.948 (1)	4.0 (7)	1.05 (5)
H142	0.503 (2)	0.117 (3)	0.945 (1)	5.4 (7)	1.08 (5)
H143	0.616 (2)	0.091 (2)	0.992 (1)	5.4 (7)	1.19 (5)

Notes: (*a*) For C and N atoms, equivalent thermal parameters (Å^2) are derived from refined anisotropic thermal parameters by the formula $B_{eq} = (4/3)\sum_i\sum_j\beta_{ij}\mathbf{a}_i.\mathbf{a}_j$. For H atoms, refined isotropic thermal parameters, B (Å^2), are given. (*b*) Electron populations (e) have been rescaled after refinement to yield neutral molecules.

viewer are shaded. Directions are given in the figure caption for copying Fig. 3 onto a transparent sheet and positioning the copy over the original in order to visualize the juxtaposition of molecules in adjacent layers of the crystal structure.

Discussion

A central question in this study is: *How does the structure of a polarizable molecule such as DMAPF change on going from the gas phase to the crystalline environment?* This question can be considered through a comparison of the X-ray structure with the geometry-optimized *ab initio* molecular orbital structure. It should be noted that X-ray bond lengths are measures of distances between the centroids of

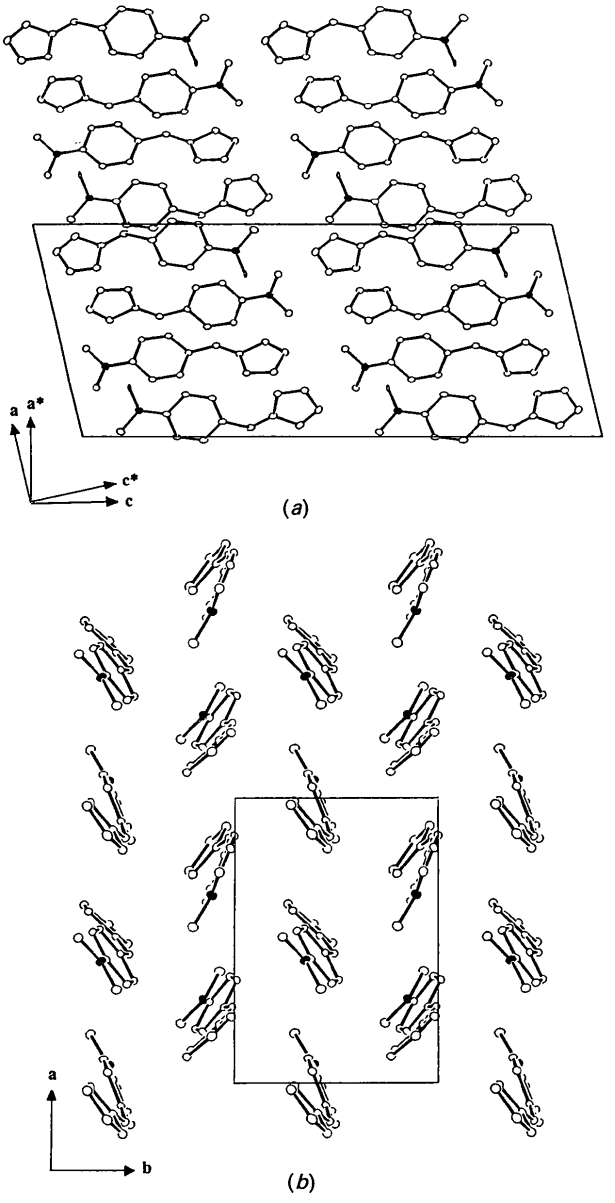

Fig. 2. Crystal packing with thermal ellipsoids at the 20% probability level (Johnson, 1976). Hydrogens are omitted and nitrogens are shaded. (*a*) View along the *b* axis with one unit cell in the *ac* plane outlined. (*b*) View in the *c** direction with one-half unit cell in the *ab* plane outlined.

Table 3. *Selected bond lengths* (Å) *for three geometries of DMAPF*

	Molecule *A*	Molecule *B*	Optimized geometry
C1—C2	1.358 (3)	1.357 (3)	1.326
C1—C5	1.463 (3)	1.463 (3)	1.491
C2—C3	1.455 (3)	1.463 (3)	1.487
C3—C4	1.342 (3)	1.342 (3)	1.325
C4—C5	1.466 (3)	1.475 (3)	1.492
C5—C6	1.364 (3)	1.362 (2)	1.331
C6—C7	1.451 (3)	1.456 (2)	1.491
C7—C8	1.408 (3)	1.410 (2)	1.394
C7—C12	1.413 (3)	1.409 (2)	1.396
C8—C9	1.374 (3)	1.377 (3)	1.382
C9—C10	1.417 (3)	1.419 (2)	1.399
C10—C11	1.411 (3)	1.412 (2)	1.401
C10—N1	1.373 (2)	1.376 (2)	1.444
C11—C12	1.370 (3)	1.376 (3)	1.379
C13—N1	1.449 (3)	1.446 (3)	1.481
C14—N1	1.456 (3)	1.455 (3)	1.481

Table 4. *Selected valence angles* (°) *for three geometries of DMAPF*

	Molecule *A*	Molecule *B*	Optimized geometry
C5—C1—C2	107.8 (2)	108.4 (2)	108.6
C1—C2—C3	109.3 (2)	108.9 (2)	109.3
C2—C3—C4	108.6 (2)	108.8 (2)	108.9
C3—C4—C5	108.8 (2)	108.8 (2)	108.9
C4—C5—C1	105.5 (2)	105.2 (2)	104.2
C4—C5—C6	121.9 (2)	121.8 (2)	124.7
C1—C5—C6	132.6 (2)	132.9 (2)	131.0
C5—C6—C7	131.9 (2)	132.5 (2)	128.7
C6—C7—C8	125.8 (2)	127.0 (2)	123.4
C6—C7—C12	117.7 (2)	116.9 (2)	119.3
C8—C7—C12	116.5 (2)	116.1 (2)	117.2
C7—C8—C9	121.7 (2)	122.1 (2)	121.5
C8—C9—C10	121.3 (2)	121.1 (2)	121.1
C9—C10—C11	117.4 (2)	117.3 (2)	117.5
C9—C10—N1	121.7 (2)	121.9 (2)	121.3
C11—C10—N1	120.9 (2)	120.8 (2)	121.2
C10—C11—C12	120.6 (2)	120.5 (2)	120.9
C7—C12—C11	122.5 (2)	122.9 (2)	121.8
C10—N1—C13	120.1 (2)	121.2 (2)	116.1
C10—N1—C14	119.7 (2)	119.8 (2)	116.1
C13—N1—C14	118.8 (2)	118.8 (2)	112.8

Table 5. *Selected torsion angles* (°) *for three geometries of DMAPF*

	Molecule *A*[a]	Molecule *B*[b]	Optimized geometry
C1—C5—C6—C7	+3.3 (4)	0.0 (4)	+3.0
C4—C5—C6—C7	−177.0 (2)	+175.0 (2)	−178.8
C5—C6—C7—C8	+13.2 (3)	+13.3 (3)	+34.1
C5—C6—C7—C12	−166.9 (2)	−165.7 (2)	−147.6
C9—C10—N1—C13	−9.0 (3)	−7.0 (3)	−23.7
C9—C10—N1—C14	−175.0 (2)	+178.6 (2)	−159.7
C11—C10—N1—C13	+171.9 (2)	+174.9 (2)	+160.1
C11—C10—N1—C14	+6.0 (3)	+0.5 (3)	+24.2

Notes: (*a*) Based on *x*, *y*, *z* cordinates. (*b*) Based on $-x$, $-y$, $-z$ coordinates.

Table 6. *Selected geometric features of DMAPF molecules*

Angles in °, distances in Å.

	Molecule *A*	Molecule *B*	Optimized geometry
Angle between least-squares planes[a]			
Aryl/Fulvene	15.3 (1)	15.6 (1)	35.4
Aryl/NMe_2	12.2 (2)	3.6 (1)	34.9
Pyramidalization[b]			
at N1	12.1 (1)	4.8 (1)	38.3
at C5	0.3 (1)	3.7 (1)	1.3
at C7	0.1 (1)	0.8 (1)	1.4
Sum of 'bay' angles (C1—C5—C6, C5—C6—C7, C6—C7—C8)	390.3 (3)	392.4 (3)	383.1
H1···H8 intramolecular distance	2.12 (3)[c]	2.12 (3)[c]	2.25
Bond-length averages			
Fulvene 'double' bonds (C1—C2, C3—C4, C5—C6)	1.355 (2)	1.354 (2)	1.327
Fulvene 'single' bonds (C1—C5, C2—C3, C4—C5)	1.461 (2)	1.467 (2)	1.490
Aryl 'double' bonds (C8—C9, C11—C12)	1.372 (2)	1.377 (2)	1.381
Aryl 'single' bonds (C7—C8, C7—C12, C9—C10, C10—C11)	1.412 (1)	1.413 (1)	1.398

Notes: (*a*) Least-squares-plane calculations based on C1, C2, C3, C4 and C5 of the fulvene ring, C7, C8, C9, C10, C11 and C12 of the aryl ring, and N1, C13 and C14 of NMe_2. (*b*) Pyramidalization at an atom bonded to three others is calculated as the average of three angles, each formed by one of the three bonds to the plane of the other two. (*c*) These values apply to the structure *before* optimization of the C—H bond lengths; after optimization, the H1···H8 distances are 2.02 Å in molecule *A* and 2.01 Å in molecule *B*.

Table 7. *Selected electronic features of isolated DMAPF molecules*

	A[a]	*B*[a]	Optimized[b]
Total charges (e)			
Fulvene ring	−0.118	−0.112	−0.064
C6 + H6	+0.040	+0.038	+0.027
Aryl ring	+0.074	+0.073	+0.071
NMe_2	+0.004	+0.002	−0.033
Approximate π charges (e)			
Fulvene ring	−0.150	−0.144	−0.081
C6	+0.089	+0.085	+0.058
Aryl ring	−0.099	−0.101	−0.072
Dipole moment[c] (D)	4.20	4.15	2.09

Notes: (*a*) Electronic charges are derived from HF/STO-3G calculations on the crystalline molecular geometries with all C—H bond lengths optimized. (*b*) Electronic charges are derived from HF/STO-3G calculations on the molecular geometry after full optimization at the HF/STO-3G level. (*c*) Dipole moments here are based on the HF/STO-3G calculations. The experimental dipole moment of DMAPF in benzene is 3.65 D (Kresze & Goetz, 1957).

electron density, whereas theoretical bond lengths give the internuclear distances between the global minima on the potential-energy surface. Nevertheless, the average C—C bond length, $r(CC)_{av}$, in molecules *A* and *B* is only 0.001 Å greater than $r(CC)_{av}$ in the optimized molecule. We therefore compare the X-ray and optimized structures of DMAPF with caution in order to analyze the effects of the crystalline environment.

The longitudinal polarization of DMAPF can be represented by resonance forms (1*a*) and (1*b*). Form (1*a*) represents through-resonance donation of π-electron density from the dimethylamino group to the fulvene ring. Form (1*b*) represents polarization of the fulvene π system by the occupied π orbitals of the benzenoid ring. The latter polarization mechanism has been invoked by Sardella *et al.* (1984) to explain the ^{13}C NMR chemical shifts of the more-twisted 6-methyl-6-arylfulvenes. Its contribution is distinguished by a downfield shift (loss of π-electron density) of the NMR peak for C6 on changing from π-electron acceptors to donors at the *para* position of the aryl ring.

As seen in Table 6, there are some major differences between the optimized conformation and those in the crystal. Thus the interplanar angle between the least-squares planes of the fulvene and aryl rings

Table 8. *Intermolecular* C···H *and* N···H *distances* <3 Å *in the crystal structure of DMAPF*

Distances were calculated before optimization of C—H bond lengths.

Non-H atom of central molecule[a]	H atom of neighboring molecule[b]	Distance (Å)
Molecule *A*		
C1	H11 of *A* (ii)	2.85 (2)
C4	H2 of *B* (iii)	2.92 (2)
C4	H133 of *B* (iv)	2.97 (2)
C5	H2 of *B* (iii)	2.78 (2)
C7	H1 of *B* (iii)	2.94 (2)
C8	H12 of *A* (ii)	2.85 (2)
C8	H1 of *B* (iii)	2.96 (2)
C10	H9 of *B* (iii)	2.96 (2)
C13	H131 of *B* (iii)	2.95 (3)
N1	H9 of *B* (iii)	2.92 (2)
N1	H131 of *B* (iii)	2.99 (3)
Molecule *B*		
C1	H11 of *B* (v)	2.78 (2)
C2	H11 of *B* (v)	2.95 (2)
C4	H1 of *A* (iii)	2.88 (2)
C7	H12 of *B* (v)	2.95 (2)
C8	H12 of *B* (v)	2.83 (2)
C10	H133 of *A* (iii)	2.75 (2)
C11	H133 of *A* (iii)	2.90 (2)
N1	H4 of *B* (v)	2.73 (2)

Notes: (*a*) Intermolecular distances are tabulated for non-H atoms in molecules of symmetry code (i) x, y, z. (*b*) Symmetry codes: (ii) $-x, \frac{1}{2}+y, \frac{3}{2}-z$; (iii) $1-x, y-\frac{1}{2}, \frac{3}{2}-z$; (iv) $x-1, y, z$; (v) $1-x, \frac{1}{2}+y, \frac{3}{2}-z$.

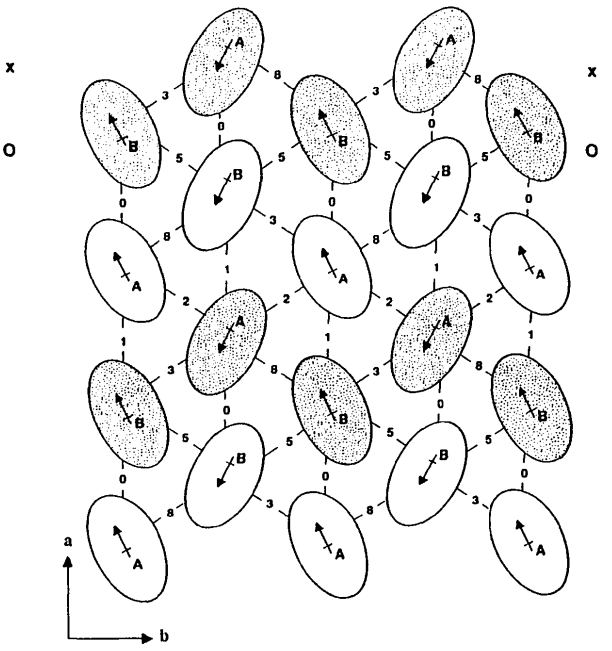

Fig. 3. Schematic drawing showing the end-on view of *A* and *B* molecules with herringbone packing as viewed along the c^* direction. Molecules with NMe_2 toward the viewer are shaded. The lateral dipole moment of each molecule and numbers of C···H and N···H contacts <3 Å between pairs of molecules are indicated. To visualize the relationship of this layer to adjacent layers, photocopy or trace this figure onto a transparent sheet, flip the copy left to right (reflection normal to *b*) and apply either a downward shift ($+c/2$) to match the Xs of the copy with the Os of the original or an upward shift ($-c/2$) to match the Xs of the original with the Os of the copy.

decreases from 35.4° in the optimized structure to 15.3 (1) and 15.6 (1)° in the two molecules of the crystal structure. This arises primarily through a reduced degree of twist about C6—C7 (Table 5). Furthermore, the pyramidalization of the N atom decreases from 38.3° (optimized) to 12.1 (1) and 4.8 (1)° for *A* and *B*, repectively, in the crystal. This difference in nitrogen pyramidalization is also reflected in the angle between the aryl and dimethylamino least-squares planes of the optimized and crystalline molecules (Table 6).

Both of these changes indicate a flattening of DMAPF that is consistent with a greater contribution of (1*a*) and/or (1*b*) to the molecules in the crystal relative to the optimized structure. Flattening causes a greater degree of crowding in the 'bay region', defined by C1, C5, C6, C7 and C8. This crowding is manifested by a reduction in the H1···H8 distance from 2.25 Å in the optimized structure to 2.12 (3) Å in both *A* and *B*. However, an even more severe crowding is avoided through an increase in the sum of the C—C—C bond angles in this region (∠C1—C5—C6, ∠C5—C6—C7 and ∠C6—C7—C8) from 383.1° in optimized DMAPF to 390.3 (3) and 392.4 (3)° in *A* and *B*, respectively (Table 6).

Bond lengths

Comparison of the bond lengths for *A* and *B* in the crystal with the optimized bond lengths (Tables 3 and 6) indicates that the differences are fully consistent with an increased contribution of resonance form (1*a*) in the crystal. Key comparisons are for the two C—C bonds involving C6 which show differences (averaged over *A* and *B*) of $+0.032$ Å for *r*(C5C6) and -0.038 Å for *r*(C6C7) in the molecules of the crystal structure relative to those of the optimized molecule. Note that C5—C6 is lengthened by the contributions of both (1*a*) and (1*b*) whereas C6—C7 is shortened only by the contribution of (1*a*). Thus, the observation that *r*(C6C7) appears to be decreased more than *r*(C5C6) is increased suggests that (1*a*) plays a major role in the crystal. However, it is probable that (1*b*) also makes a contribution considering the lower force constant for shortening a single bond than for lengthening a double bond.

Other bond-length differences between the optimized and the crystal structure are also consistent with a greater polarization of DMAPF in the crystal. Thus the single- and double-bond lengths in the fulvene moiety change by averages of -0.026 and $+0.028$ Å, respectively [consistent with increased contributions by (1*a*) and (1*b*)] and the aryl ring is altered toward a more quinoid form (as in 1*a*) with bond-length changes averaging 0.011 Å. The shortening observed for the *N*-methyl bonds of *A* and *B* is consistent with both a decrease in the

pyramidalization of the nitrogen, resulting in a rehybridization of N from nominally sp^3 in the optimized structure ($\angle$C13—N—C14 = 112.8°) to nominally sp^2 in the crystal [$\angle$C13—N—C14 = 118.8 (2)°], and with an increase in π delocalization in *A* and *B*.

π-Electron distribution

As seen in Table 7, the π charges in the fulvene ring of the *A* and *B* molecules, as derived from molecular orbital calculations on the isolated molecules, are *ca* 0.06 e more negative than in the fulvene ring of optimized DMAPF, whereas the π charge at C6 is *ca* 0.03 e more positive. This suggests enhanced contributions from both (1*a*) and (1*b*) in isolated *A* and *B* owing to the more coplanar arrangement of the five- and six-membered rings. In addition, the π charge in the aryl ring is *ca* 0.03 e more negative in *A* and *B*, a result consistent with a greater degree of π donation from dimethylamino groups that are less pyramidalized than in the optimized structure. These charge differences are reflected in a calculated dipole moment more than 2 D larger for the isolated *A* or *B* molecule than for the optimized geometry (Table 7).

Because of the polarizability of DMAPF, *A* and *B* are expected to be much more polar in the crystalline environment than as isolated molecules. Considering that the dipole moment of DMAPF in the nonpolar (but polarizable) solvent benzene (3.65 D) is 75% greater than that calculated for the optimized molecule (corresponding to the gas phase) (Table 7), the dipole moment in the crystal is undoubtedly much greater than in benzene. Indications of increased polarity in the crystal have recently been reported for several compounds by Spackman, Weber & Craven (1988).

Comparison of the A and B molecules

Although most of the structural differences between molecules *A* and *B* are within experimental uncertainties, those differences that are statistically significant are generally consistent with isolated *A* being slightly more polar than isolated *B*. Thus C6—C7 and the average fulvene single bond are shorter in *A* than in *B* and C5—C6 is longer in *A* than in *B*. *A* is calculated to have a larger dipole moment than *B* (Table 7), even though the dimethylamino group is more pyramidal in *A*. One of the more interesting structural differences is that C5 and C7 of *B* are pyramidalized in the same direction by 3.7 (2) and 0.8 (2)°, respectively, whereas these atoms and their substituents are essentially planar within experimental error in *A*. Thus, *A* is more or less linear while *B* is distinctly curved in shape when viewed from the side, as shown in *ORTEP* drawings (with H atoms omitted) in Fig. 4. The difference in curvature is emphasized in Fig. 4 by an added line that is collinear with C5—C6 of each molecule.

Lateral polarization

In addition to longitudinal polarization of electron density toward the fulvene end of DMAPF, there is also polarization toward the 'bay' side of each molecule in the crystalline environment. The total charge on atoms along this side (C1, C2, C5, C7, C8, C9, C13 plus the hydrogens bonded to them) and the charge on atoms along the opposite side (C3, C4, C6, C11, C12, C14 plus hydrogens) can be calculated from electron populations derived from the diffraction data (Table 2). For molecule *A*, the sums of atomic charges are −0.7 (2) and +0.8 (2) e along the bay side and the opposite side, respectively. For molecule *B*, the sums are −0.3 (2) and +0.3 (2) e, again corresponding to polarization of electron density toward the bay side of the molecule. This lateral polarization, indicated by arrows on each molecule in Fig. 3, is important for understanding the crystal packing of DMAPF.

Packing within layers

Each layer in the *ab* plane contains molecules arranged so that an end-on view of the molecules in one layer presents a herringbone pattern, as shown in Figs. 2(*b*) and 3. The number of close encounters between neighboring molecules is indicative of the magnitude of the intermolecular interaction. As can be seen in Fig. 3, nearly all of the intermolecular C···H and N···H distances that are <3 Å are between the side of one oval and the end of another. These are primarily attractive overlaps between π-electron-rich faces and electron-depleted H atoms on the edges of the five- and six-membered rings. Similar interactions are a common feature of the crystal packing of aromatic molecules (Glusker & Trueblood, 1985; Gavezzotti & Desiraju, 1988).

If one carries out the procedure described in the caption of Fig. 3, one can see diagonal sheets of

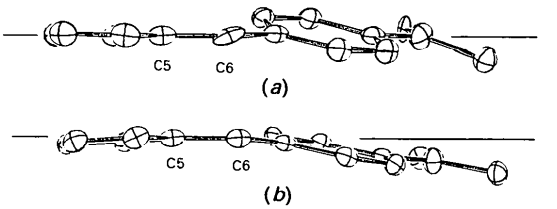

Fig. 4. Edge view of molecules *A* and *B* normal to the plane defined by C4, C5 and C6 of each molecule with thermal ellipsoids at the 50% probability level and hydrogens omitted (Johnson, 1976). A horizontal line is drawn collinear with the C5—C6 bond of each molecule. (*a*) Molecule *A*, *x*, *y*, *z* coordinates. (*b*) Molecule *B*, $-x, -y, -z$ coordinates.

molecules with the NMe_2 group oriented alternately into or out of the diagram. These sheets lie along one diagonal if the copy is shifted downward (positive along the c axis) and along the other diagonal if the copy is shifted upward (negative along the c axis). This packing arrangement suggests that crystal growth occurs along the diagonals of the unit cell in the ab plane due to favorable lengthwise dipole–dipole interactions. The final position of each molecule with respect to its side-by-side neighbors allows positive and negative regions of electrostatic potential to overlap. The edge-to-face arrangement between aromatic rings contributes to this overlap and yields the herringbone pattern seen in Figs. 2(*b*) and 3.

Packing between layers

There are four different molecular 'ends' at each layer surface, the dimethylamino ends (NMe_2) of *A* and *B* molecules, and the fulvene ends of *A* and *B* molecules. Each of these fits into a niche formed by the ends of three molecules in the next layer, as listed in Table 9. Note that the NMe_2 group of *A* has two NMe_2 neighbors (one *A* and one *B*) in the adjacent layer whereas NMe_2 of *B* has only one (an *A* molecule). This may be related to the nitrogen pyramidalization being greater in *A* than in *B*, since the NMe_2 group of *A* is more crowded by its neighbors than is NMe_2 of *B*.

Owing to the longitudinal polarization of each molecule, the dimethylamino group carries a partial positive charge and the fulvene ring a partial negative charge that can be expected to contribute to attractive and repulsive forces between layers. However, it can be seen in Table 9 that the numbers of attractive and repulsive interactions are equal; thus, longitudinal polarization of DMAPF molecules in the crystal does not account for interlayer cohesion in a simple manner.

The lateral polarization of these molecules does provide a mechanism for interlayer cohesion. This is a consequence of the bay sides of *all* of the molecules in one layer being oriented toward either $+b$ or $-b$ so that the direction of the lateral component of the molecular dipole moment alternates from $+b$ in one layer to $-b$ in the next.

This research has been supported by NSF grants CHE-8604007 and CHE-8618756 to SWS. We thank Robert Stewart, Jeffrey Strnad, Todd Williamson and Steven Lee, of Carnegie Mellon Univeristy, and John Ruble, University of Pittsburgh, for their valuable technical assistance.

Table 9. *End-to-end interlayer interactions between DMAPF molecules*

	Closest end groups of molecules in adjacent layer	
End group	With same charge	With opposite charge
NMe_2 of *A*	NMe_2 of *A*, NMe_2 of *B*	Fulvene of *A*
NMe_2 of *B*	NMe_2 of *A*	Fulvene of *A*, fulvene of *B*
Fulvene of *A*	Fulvene of *B*	NMe_2 of *A*, NMe_2 of *B*
Fulvene of *B*	Fulvene of *A*, fulvene of *B*	NMe_2 of *B*
Total	Six repulsive interactions	Six attractive interactions

References

BARON, P. A., BROWN, R. D., BURDEN, F. R., DOMAILLE, P. J. & KENT, J. E. (1972). *J. Mol. Spectrosc.* **43**, 401–410.

BLESSING, R. H. (1987). *Crystallogr. Rev.* **1**, 3–58.

BÖNZLI, P., OTTER, A., NEUENSCHWANDER, M., HUBER, H. & KELLERHALS, H. P. (1986). *Helv. Chim. Acta*, **69**, 1052–1064.

DETITTA, G. T. (1985). *J. Appl. Cryst.* **18**, 75–79.

FRISCH, M. J., HEAD-GORDON, M., SCHLEGEL, H. B., RAGHAVACHARI, K., BIRKLEY, J. S., GONZALEZ, C., DEFREES, D. J., FOX, D. J., WHITESIDE, R. A., SEEGER, R., MELIUS, C. F., BAKER, J., MARTIN, R. L., KAHN, L. R., STEWART, J. J. P., FLUDER, E. M., TOPOIL, S. & POPLE, J. A. (1988). *GAUSSIAN*88. Gaussian Inc., Pittsburgh, PA, USA.

GAVEZZOTTI, A. & DESIRAJU, G. R. (1988). *Acta Cryst.* B**44**, 427–434.

GLUSKER, J. P. & TRUEBLOOD, K. N. (1985). *Crystal Structure Analysis*, p. 172. Oxford Univ. Press.

HEHRE, W. J., DITCHFIELD, R., STEWART, R. F. & POPLE, J. A. (1970). *J. Chem. Phys.* **52**, 2769–2773.

HEHRE, W. J., STEWART, R. F. & POPLE, J. A. (1969). *J. Chem. Phys.* **51**, 2657–2664.

IKEDA, H., KAWABE, Y., SAKAI, T. & KAWASAKI, K. (1989). *Chem. Phys. Lett.* **157**, 576–578.

JOHNSON, C. K. (1976). *ORTEP*II. Report ORNL-5138. Oak Ridge National Laboratory, Tennessee, USA.

KRESZE, G. & GOETZ, H. (1957). *Chem. Ber.* **90**, 2161–2176.

LEHMANN, M. S. & LARSEN, F. K. (1974). *Acta Cryst.* A**30**, 580–584.

MAIN, P., HULL, S. E., LESSINGER, L., GERMAIN, G., DECLERCQ, J.-P. & WOOLFSON, M. M. (1978). *MULTAN*78. *A System of Computer Programs for the Automatic Solution of Crystal Structures from X-ray Diffraction Data.* Univs. of York, England, and Louvain, Belgium.

OTTER, A., MÜHLE, H., NEUENSCHWANDER, M. & KELLERHALS, H. P. (1979). *Helv. Chim. Acta*, **62**, 1626–1631.

REPLOGLE, E. S., TRUCKS, G. W. & STALEY, S. W. (1991). *J. Phys. Chem.* **95**, 6908–6912.

SARDELLA, D. J., KEANE, C. M. & LEMONIAS, P. (1984). *J. Am. Chem. Soc.* **106**, 4962–4966.

SCHARPEN, L. H. & LAURIE, V. W. (1965). *J. Chem. Phys.* **43**, 2765–2766.

SCHLEGEL, H. B. (1982). *J. Comput. Chem.* **3**, 214–218.

SPACKMAN, M. A. (1987). Personal communication.

SPACKMAN, M. A., WEBER, H. P. & CRAVEN, B. M. (1988). *J. Am. Chem. Soc.* **110**, 775–782.

STEWART, R. F. & SPACKMAN, M. A. (1983). *VALRAY Users Manual.* Department of Chemistry, Carnegie Mellon Univ., USA.

THIEC, J. & WIEMANN, J. (1956). *Bull. Soc. Chim. Fr.* pp. 177–180.

THIELE, J. (1900). *Chem. Ber.* **33**, 666–673.

THIELE, J. & BALHORN, H. (1906). *Liebigs Ann. Chem.* **348**, 1–15.

WHELAND, G. W. & MANN, D. E. (1949). *J. Chem. Phys.* **17**, 264–268.